Excitons and Optical Properties of α-Quartz

Eric K. Chang,[1] Michael Rohlfing,[2] and Steven G. Louie[1]
[1]Department of Physics, University of California at Berkeley, Berkeley, California 94720
and Materials Science Division, Lawrence Berkeley National Laboratory, Berkeley, California 94720
[2]Institut für Theoretische Physik II, Universitaät Münster, Münster, Germany 48149

(Received 10 April 2000)

We present an *ab initio* study of the optical properties of α-quartz. The absorption spectrum is calculated by solving the Bethe-Salpeter equation for the interacting electron-hole system and found to be in excellent agreement with the measured spectrum up to 10 eV above the absorption threshold. We find that excitonic effects are crucial in understanding the sharp features in the absorption spectrum in this energy range. They are also crucial in the *ab initio* computation of the static dielectric constant, significantly enhancing its value.

PACS numbers: 78.20.Ci, 71.35.Cc

The optical, electronic, and structural properties of quartz have been measured and studied extensively by experimentalists. In particular, Philipp [1] has performed measurements of the reflectance of light normal to the surface of quartz in an energy range from 0 to 30 eV. The measured optical absorption shows four sharp and distinct peaks at energies of 10.3, 11.7, 14.0, and 17.3 eV, respectively. In the past thirty years, many theoretical studies [2–5] have been done in an attempt to explain the origin of these peaks. These studies considered either interband transitions alone or excitonic formation within a model Hamiltonian approach. In the interband theory, the optical absorption is computed using Fermi's golden rule and neglecting the electron-hole interaction. Chelikowsky and Schluter [2] used the interband theory approach with an empirical band structure. Xu and Ching [3] used the same approach, but calculated the band structure within the local density approximation (LDA). According to the interband transition picture, only the first peak is attributed to excitons whereas the other higher peaks arise from Van Hove singularities in the joint density of states (JDOS), enhanced by matrix element effects. In the model exciton approach of Pantelides [4] and Laughlin [5], the optical absorption spectrum of α-quartz is computed using a tight-binding Hamiltonian and an approximate form for the two-particle Green's function. According to the former study, only the first two peaks are excitonic in nature, whereas in the latter study all four peaks are found to be excitonic in nature.

In this work, we go beyond the previous studies by using accurate *ab initio* methods at all stages of the calculation of the optical absorption, including the calculation of the quasiparticle band structure and the electron-hole interaction. Such an approach not only provides us with a more accurate optical spectrum calculated without using adjustable parameters and without making *a priori* assumptions about the nature of the peaks, but also gives us additional information about the physical and spatial nature of the excitons in the system, thereby deepening our understanding of the optical excitations in this technologically important material.

The theoretical method used in this work is based on the approach developed by Rohlfing and Louie [6], which has been applied successfully to the optical absorption spectrum of a wide variety of semiconductors and insulators, including surfaces, clusters, and polymer systems [7,8]. Similar approaches with different methods have been used by others to investigate the optical properties of solids [9,10].

In the calculation, the relevant electron-hole excited states are described approximately by the following many-body wave function:

$$|E\rangle = \sum_{cv\mathbf{k}} A_{cv\mathbf{k}} a^{\dagger}_{c\mathbf{k}} a_{v\mathbf{k}} |G\rangle , \tag{1}$$

where $|E\rangle$ and $|G\rangle$ are the excited and ground states, respectively, and c, v, and $\mathbf{k}$ label the conduction bands, valence bands, and $\mathbf{k}$ vectors of the quasiparticle states. $a^{\dagger}_{c\mathbf{k}}$ and $a_{v\mathbf{k}}$ are the operators corresponding to the creation of an electron and a hole, respectively. The coefficients $A_{cv\mathbf{k}}$ contain the information about electron-hole correlation and the spatial nature of the excited state to which $|E\rangle$ corresponds. We are interested in such linear superpositions of vertical transitions, because the momentum of the optical photon absorbed by the system is small compared to the size of the first Brillouin zone (and hence, we need only be concerned with vertical transitions for zero temperature); furthermore, the intensity of light in the experiments we aim to explain is small enough so that one-photon absorption processes are dominant (as opposed to higher-photon processes).

The coefficients $A_{cv\mathbf{k}}$ satisfy the following secular equation known as the Bethe-Salpeter equation (BSE) [11]:

$$(E^{\mathrm{QP}}_{c\mathbf{k}} - E^{\mathrm{QP}}_{v\mathbf{k}}) A_{cv\mathbf{k}} + \sum_{v'c'\mathbf{k}'} K^{c'v'\mathbf{k}'}_{cv\mathbf{k}} A_{c'v'\mathbf{k}'} = \Omega A_{cv\mathbf{k}} , \tag{2}$$

where the $\{E^{\mathrm{QP}}\}$ are the quasiparticle energies, i.e., the energies required to add or subtract an electron. In practice, we compute these quasiparticle energies in the *GW* approximation [12,13], which has been shown to yield accurate results for a wide variety of semiconductors and insulators. Ω is the energy of the coupled electron-hole excitation, and $K^{c'v'\mathbf{k}'}_{cv\mathbf{k}}$ describes the scattering of an electron hole in the configuration $cv\mathbf{k}$ to the configuration $c'v'\mathbf{k}'$ via the Coulomb interaction. The kernel $K^{c'v'\mathbf{k}'}_{cv\mathbf{k}}$ is in general a complicated expression which may be expressed as an infinite sum over irreducible Feynman diagrams or as a sum of functional derivatives of the Hartree energy and electron self-energy with respect to the single-particle Green's function. We take $K = 2K_x + K_d$, which is the appropriate expression for spin-singlet, optically excitable states [11,14]. K_x is the exchange interaction and K_d is the attractive, screened direct Coulomb interaction between electron and hole; both can be evaluated from a knowledge of the quasiparticle wave functions and screened Coulomb interaction [6].

Once the Bethe-Salpeter equation [Eq. (2)] is solved, we may use the coefficients $A^{(s)}_{cv\mathbf{k}}$ and the energies Ω_s to compute both the excitonic wave functions in real space, $\Psi_s(r, r')$, and the optical absorption spectrum, $\epsilon_2(\omega)$. They are given by (in atomic units)

$$\epsilon_2(\omega) = \frac{4\pi}{\omega^2}\sum_s \left|\sum_{cv\mathbf{k}} A^s_{cv\mathbf{k}}\langle c\mathbf{k}|\mathbf{V}\cdot\hat{e}|v\mathbf{k}\rangle\right|^2 \delta(\omega - \Omega_s) \tag{3}$$

(where $\mathbf{V}$ and $\hat{e}$ are the velocity operator and the polarization vector, respectively), and

$$\Psi_s(\mathbf{r_e}, \mathbf{r_h}) = \sum_{cv\mathbf{k}} A^{(s)}_{cv\mathbf{k}}\phi_{c\mathbf{k}}(\mathbf{r_e})\phi^*_{v\mathbf{k}}(\mathbf{r_h})\,. \tag{4}$$

The quasiparticle energies of α-quartz calculated in the *GW* approximation are shown in Fig. 1. We note that the nearly direct gap at Γ is opened up significantly from the LDA value of 5.6 eV to a value of 10.1 eV. The top twelve valence bands correspond to p-like oxygen lone-pair states. The bottom conduction bands have both silicon and oxygen s and p characters.

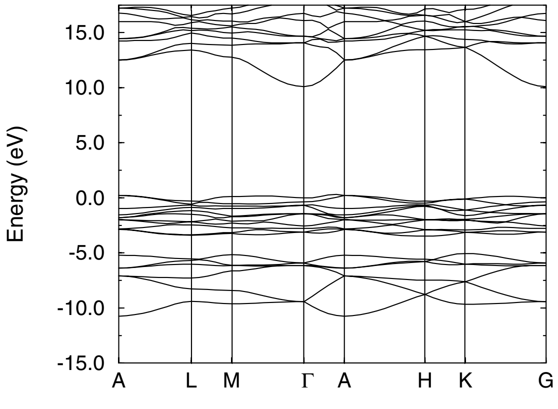

FIG. 1. Calculated quasiparticle band structure of α-quartz in the *GW* approximation.

α-quartz is birefringent, i.e., the optical constants for rays parallel to the hexagonal plane are different from those perpendicular to the plane. In this work, we are concerned with the perpendicular ray, the so-called "ordinary ray," which is the one used in experiment [1]. We therefore take our polarization vector $\hat{e}$ in our expression for $\epsilon_2(\omega)$ [see Eq. (3)] to be in the hexagonal plane.

In previous calculations of the direct kernel K^d for other materials, the screening has been computed in the random phase approximation (RPA) ignoring exciton effects, i.e., ignoring the fact that the virtual hole and electron interact. The RPA screening has worked quite well for small and moderate-size band gap semiconductors. In α-quartz, however, excitons may have a significant effect on the dielectric screening since α-quartz is a wide band gap insulator with a large excitonic binding energy. Since such effects are ignored in the RPA dielectric function, we need to use the following expression instead, which takes into account the virtual electron-hole interaction and is a better approximation to the screening than the RPA:

$$\chi^{\mathrm{RPA+ex}} = 2\sum_s \frac{1}{\Omega_s^3}\left|\sum_{cv\mathbf{k}} A^{(s)}_{cv\mathbf{k}}\langle c\mathbf{k}|\hat{e}\cdot\mathbf{V}|v\mathbf{k}\rangle\right|^2. \tag{5}$$

Here $\chi^{\mathrm{RPA+ex}}$ is the macroscopic polarizability computed with exciton effects included. Including the effects of local fields, we get a macroscopic dielectric constant of 2.0, in the case of RPA, and 2.44, in the case of RPA + excitons. The latter is in excellent agreement with the experimental value of 2.38 [15].

Since solving the excitonic coefficients $A_{cv\mathbf{k}}$ requires knowledge of the dielectric screening $\chi^{\mathrm{RPA+ex}}$, and vice versa, the BSE together with Eq. (5) is a system of equations that needs to be solved self-consistently by an iterative scheme. Each iteration consists of a calculation of $\chi^{(n)}$, given an approximate value of the coefficients $A^{(n)}_{cv\mathbf{k}}$. The dielectric screening is then used in the BSE to compute an updated set of coefficients $A^{(n+1)}_{cv\mathbf{k}}$, which are substituted into Eq. (5) to obtain an updated screening $\chi^{(n+1)}$. This process is iterated to convergence. If we take as an initial guess, $A^{(n)}_{cv\mathbf{k}} = \delta_{cc'}\delta_{vv'}\delta_{\mathbf{k}\mathbf{k}'}$ with c', v', and $\mathbf{k}'$ running over all conduction, valence, and $\mathbf{k}$ vectors, and $\chi^{(0)} = \chi^{\mathrm{RPA}}$, then only two iterations are required for α-quartz until convergence is reached. For many semiconductor materials, such an elaborate iterative scheme is however not required [6–10].

The large difference between the RPA and RPA + exciton dielectric constants effects a significant change in the resulting optical spectrum as can be seen in Fig. 2(a). We notice that the first two peaks are systematically shifted to higher energy. In particular, the peak positions are shifted by 0.5 eV towards the corresponding experimental peaks, and the peak heights are appreciably lowered.

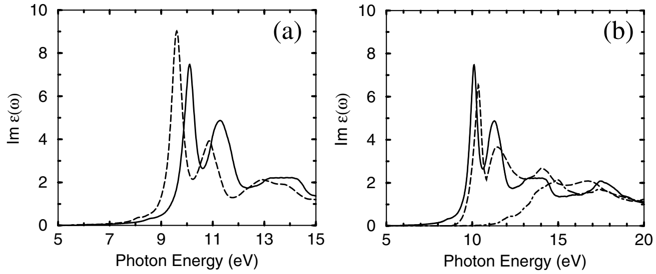

FIG. 2. (a) Absorption spectrum with excitonic effects calculated with RPA (dashed line) and with RPA + excitons (solid line) dielectric screening. (b) Absorption spectrum with excitonic effects calculated with RPA + excitons (solid line) screening as compared to the interband theory (dot-dashed line). Experimental data are given by the dashed line.

In Fig. 2(b) we plot the spectrum from 5 to 20 eV. The positions of the four peaks computed theoretically are located at 10.1, 11.3, 13.5, and 17.5 eV, in excellent agreement with the experimental values of 10.3, 11.7, 14.0, and 17.3 eV. The first two peaks are clearly excitonic in nature, since the absorption without excitonic effects is nearly featureless in the interval from 0 to 15 eV. The third and fourth peaks, if compared to the interband transition spectrum, show a strong excitonic component. This resolves the long-standing controversy over the nature of these peaks, which, being excitonic in nature, cannot be explained by interband transitions.

From the eigenvalues Ω_s obtained from diagonalizing the BSE, we compute the density of excitations, $D_{\mathrm{ex}}(\omega) = \sum_s \delta(\omega - \Omega_s)$, which we compare directly to the JDOS, $D_{\mathrm{jdos}}(\omega) = \sum_{vc\mathbf{k}} \delta(\omega - E^{\mathrm{QP}}_{c\mathbf{k}} + E^{\mathrm{QP}}_{v\mathbf{k}})$, i.e., the density of excitations with the electron-hole interaction turned off. These results are plotted in Fig. 3. We note that both are quite similar. This leads us to conclude that the sharp peaks in the optical absorption are due to enhanced oscillator strength of transitions to the excitonic states. The enhancement arises from the fact that in certain excitations the electron and hole are highly correlated and form bound or resonance states.

We use Eq. (4) to look at the spatial nature of the excitonic wave functions for select excitations. To illustrate such excitations, we place the electron at a fixed point close to one of the oxygen atoms, and plot the hole probability density on the $(1\bar{1}00)$ plane. Noting the form of Eq. (4) and the oxygen p-like character of the top valence bands, we expect a plot arranged in this way to show localized lone-pair p orbitals on the oxygen atoms modulated by an envelope function which characterizes the extent of the exciton. Figure 4(a) shows the exciton of the first peak in Fig. 2(b). We note that it is a highly correlated electron-hole state with a small size not exceeding 2–3 bond lengths, and with a high electron-hole overlap probability which gives rise to a large absorption strength. Since the optical dipole matrix element depends strongly on the degree of localization of the excitation and becomes larger the more localized the excitation, the exciton associated with the first peak is very spatially localized as expected. These states however are located just at the quasiparticle continuum edge and hence, technically, they should be considered as resonant states within the accuracy of our calculation.

Figure 4(b) shows the exciton corresponding to the second peak. It is more delocalized than the exciton of the first peak. It is fairly extended along the (0001) direction, as can be seen by the fact that we get nearly undiminished intensity on certain oxygen sites that are many bond lengths away from the fixed electron.

From the solutions of the BSE, we actually find that the lowest eigenvalue state is at a significantly lower energy than the first peak at 10.1 eV. It however has very weak oscillator strength and therefore does not give rise to a peak in the optical spectrum. Its energy is 8.4 eV, 1.7 eV lower than the minimum direct band gap. It is therefore a strongly bound exciton. However, for this state, there is very little overlap between the electron and hole and hence a small optical oscillator strength for transitions to this state.

In conclusion, we succeed in calculating from first principles the optical absorption spectrum of α-quartz to 10 eV

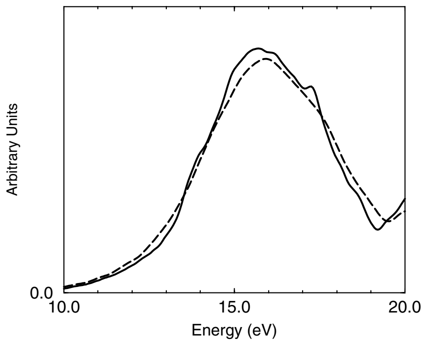

FIG. 3. Calculated density of excitons (solid line) and interband JDOS (dashed line).

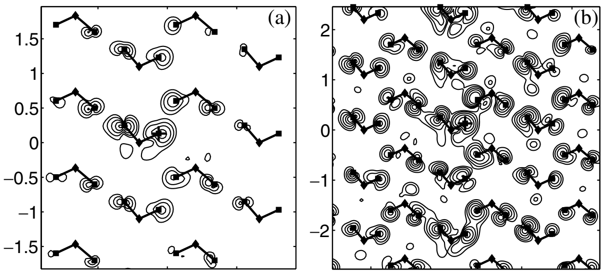

FIG. 4. A log plot of the hole probability density with the electron placed at + of (a) the first peak and (b) the second peak in the optical spectrum. The plot is in the (110) plane. The diamonds correspond to silicon atoms and the squares to oxygen atoms. The scale is in units of the lattice constant.

above the absorption threshold. The peak positions and relative peak heights are in excellent agreement with experiment. We gain insight into the physical and spatial natures of the excitons, finding two singlet excitons below or near the quasiparticle gap: one charge-transfer, "dark" exciton, and one "bright" exciton at 10.1 eV which gives rise to the first observed peak. The second observed peak is also attributable to a resonant exciton whose spatial nature is very extended along the (0001) direction. By comparing the full spectrum with the nearly featureless absorption spectrum computed neglecting excitonic effects, we conclude that all four peaks in the experimental spectrum are dominantly excitonic in nature and cannot be explained by interband transitions alone. Finally, we discover that exciton effects play an important role not only in the shape of the final absorption spectrum but also in the value of the static dielectric constant. We have performed the first *ab initio* calculation of the dielectric constant of α-quartz including electron-hole effects and obtained a value in excellent agreement with experiment. This effect is expected to be important also in the static dielectric constant of other wide band gap materials in which exciton effects are large.

This work was supported by the National Science Foundation under Grant No. DMR-9520554, and by the Office of Energy Research, Office of Basic Energy Sciences, Materials Sciences Division of the U.S. Department of Energy under Contract No. DE-AC03-76SF00098. Computer time was provided by NSF at the NCSA in Illinois. M. R. acknowledges support by the Deutsche Forschungsgemeinschaft (Grant No. Ro-1318/2-1).

[1] H. R. Philipp, Solid State Commun. **4**, 73 (1966).
[2] J. R. Chelikowsky and M. Schluter, Phys. Rev. B **15**, 4020 (1977).
[3] Y. Xu and W. Y. Ching, Phys. Rev. B **44**, 10 048 (1991).
[4] S. Pantelides, in *The Proceedings of the International Topical Conference, Yorktown Heights, NY* (Pergamon Press, New York, 1978), pp. 80–84.
[5] R. B. Laughlin, Phys. Rev. B **22**, 3021 (1980).
[6] M. Rohlfing and S. G. Louie, Phys. Rev. Lett. **81**, 2312 (1998).
[7] M. Rohlfing and S. G. Louie, Phys. Rev. Lett. **82**, 1959 (1999).
[8] M. Rohlfing and S. G. Louie, Phys. Rev. Lett. **83**, 856 (1999).
[9] L. X. Benedict, E. L. Shirley, and R. B. Bohm, Phys. Rev. Lett. **80**, 4514 (1998).
[10] S. Albrecht, L. Reining, R. Del Sole, and G. Onida, Phys. Rev. Lett. **80**, 4510 (1998).
[11] G. Strinati, Phys. Rev. Lett. **49**, 1519 (1982).
[12] L. Hedin, Phys. Rev. **139**, A796 (1965).
[13] M. Hybertsen and S. G. Louie, Phys. Rev. B **34**, 5390 (1985).
[14] A. L. Fetter and J. D. Walecka, *Quantum Theory of Many-Particle Systems* (McGraw-Hill, New York, 1971), p. 562.
[15] W. L. Wolf, S. B. Stanley, and K. A. McCarthy, *American Institute of Physics Handbook* (McGraw-Hill, New York, 1963), p. 24.